Dynamics and rheology of a dilute suspension of vesicles: Higher-order theory

Gerrit Danker, Thierry Biben, Thomas Podgorski, Claude Verdier, and Chaouqi Misbah*

Laboratoire de Spectrométrie Physique, UMR, 140 Avenue de la Physique, Université Joseph Fourier, and CNRS, 38402 Saint Martin d'Heres, France

(Received 26 March 2007; revised manuscript received 4 July 2007; published 9 October 2007)

Vesicles under shear flow exhibit various dynamics: tank treading (*TT*), tumbling (*TB*), and vacillating breathing (*VB*). The *VB* mode consists in a motion where the long axis of the vesicle oscillates about the flow direction, while the shape undergoes a breathing dynamics. We extend here the original small deformation theory [C. Misbah, Phys. Rev. Lett. **96**, 028104 (2006)] to the next order in a consistent manner. The consistent higher order theory reveals a direct bifurcation from *TT* to *TB* if $C_a \equiv \tau\dot{\gamma}$ is small enough—typically below 0.5, but this value is sensitive to the available excess area from a sphere (τ=vesicle relaxation time towards equilibrium shape, $\dot{\gamma}$=shear rate). At larger C_a the *TB* is preceded by the *VB* mode. For $C_a \gg 1$ we recover the leading order original calculation, where the *VB* mode coexists with *TB*. The consistent calculation reveals several quantitative discrepancies with recent works, and points to new features. We briefly analyze rheology and find that the effective viscosity exhibits a minimum in the vicinity of the *TT*-*TB* and *TT*-*VB* bifurcation points. At small C_a the minimum corresponds to a cusp singularity and is at the *TT*-*TB* threshold, while at high enough C_a the cusp is smeared out, and is located in the vicinity of the *VB* mode but in the *TT* regime.

DOI: 10.1103/PhysRevE.76.041905 PACS number(s): 87.16.Dg, 87.19.Tt, 83.80.Lz

I. INTRODUCTION

Vesicles are closed membranes suspended in an aqueous medium. They constitute an interesting viscoelastic model mimicking more complex entities, and they continue to receive an increasing interest both theoretically and experimentally.

Under a linear shear flow, a vesicle (where the membrane is in its fluid state) is known to exhibit a tank-treading (*TT*) motion, while its long axis makes an angle $\psi < \pi/4$ with the flow direction [1,2]. In the presence of a viscosity contrast $\lambda = \eta_1/\eta_0$ (η_1 and η_0 are the internal and external viscosities, respectively), ψ decreases until it vanishes at a critical value of $\lambda = \lambda_c$. For a small enough $C_a \equiv \tau\dot{\gamma}$ (τ is the relaxation time towards the equilibrium shape in the absence of flow, $\dot{\gamma}$ is the shear rate) the *TT* exhibits a saddle-node bifurcation towards tumbling (*TB*) [3].

Recently, a new type of motion has been predicted [4], namely, a vacillating breathing (*VB*) mode: the vesicle's long axis undergoes an oscillation (or vacillation) around the flow direction, while the shape executes a breathing motion. The three types of motion (*TT*, *TB*, and *VB*) are shown in Fig. 1.

Shortly after this theoretical prediction, an experimental report on this type of mode has been presented [5] (referred to as trembling by the authors; actually trembling may evoke some kind of noisy dynamics, and seems to us an inappropriate denomination, since the *VB* mode is periodic in time) and in Ref. [6] a qualitatively similar motion called "transition motion" in the vicinity of the *TT*-*TB* transition has been observed. Nevertheless, a detailed experimental study of this *VB* mode would be interesting but has not been reported yet. Since then, works providing further understanding [7] or attempting [8,9] to extend the original theory [4] to higher order deformation (with the aim to account for the experimental observation [5]) have been presented. Interesting features have emerged [8,9] regarding the behavior of the *VB* mode as a function of C_a.

The first aim of this paper is to present the result of the consistent theory regarding the higher order calculation. We find significant differences with recent works [8,9] regarding the form of the evolution equation. This implies, in particular, that the location of the boundaries separating the various three regimes in parameter space is significantly affected. Furthermore, by accounting properly for higher order terms, it is shown that contrary to the belief in Ref. [8] the so-called self-similarity (in that only two independent parameters survive in the final evolution equations) does not hold.

A second important report is to investigate how the effective viscosity derived recently in Refs. [4,10] is affected by the higher order deformation. In the *TT* regime the effective viscosity derived in Ref. [4] is still a decreasing function of λ and is only slightly shifted by the higher order terms. It is found that for a small enough C_a the effective viscosity of the suspension (as a function of λ) still exhibits a cusp singularity at the *TT*-*TB* bifurcation as reported in Ref. [10], while the cusp becomes a smooth minimum when C_a is high enough, namely, when the *TT*-*VB* bifurcation occurs.

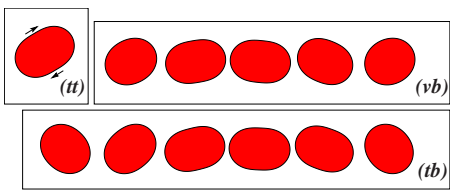

FIG. 1. (Color online) The three types of motion are shown. The arrows for the *TT* regime refer to the tank-treading motion of the membrane. Note that for the *TB* the vesicle long axis makes a full rotation by an angle π, while in the *VB* the long axis oscillates about the horizontal axis. The parameters are $\epsilon = 0.5$ and $\lambda = 2$ (*TT*), $\lambda = 9$ (*VB*), and $\lambda = 10$ (*TB*).

*chaouqi.misbah@ujf-grenoble.fr

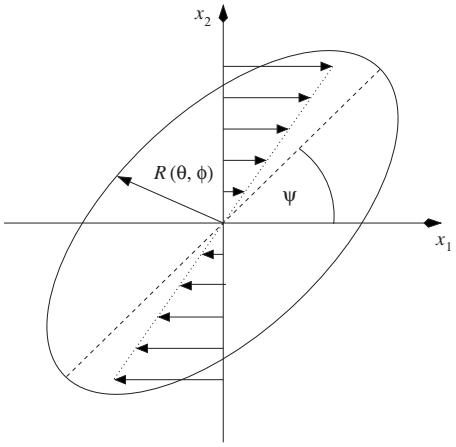

FIG. 2. Various geometrical quantities.

The scheme of the paper is as follows. In Sec. II we present in detail how a consistent calculation should be made, and develop the various necessary steps, including geometry, the calculation of the velocity field, and the treatment of the boundary conditions. Section III deals with the derivation of the leading order solution, whereas Sec. IV presents the outcome of the next order solution. The final evolution equation is presented in Sec. V, and a comparison with previous works is given in Sec. VI. Section VII is devoted to the main results of dynamics, and a brief discussion is devoted to rheology in Sec. VIII. Section IX is dedicated to a discussion and conclusion.

II. ASYMPTOTIC EXPANSION

A. Vesicle geometry

The various geometrical quantities are shown on Fig. 2. The time-dependent vesicle surface is described by $\mathbf{R}=R(\theta,\phi,t)\mathbf{e}_r$, where

$$R(\theta,\phi,t) = r_0[1 + \epsilon f(\theta,\phi,t)]. \tag{1}$$

Here r_0 is the radius of the equivalent sphere of the vesicle and ϵ is a small parameter, which can be related to the excess area Δ via $\Delta=\epsilon^2$ (with a proper expansion and normalization of f). This parameter serves formally as an expansion parameter ($\epsilon=0$ is a sphere) [7]. For the following it is convenient to rescale spatial variables by r_0, so that we are left with

$$R(\theta,\phi,t) = 1 + \epsilon f(\theta,\phi,t). \tag{2}$$

Several notations and the spirit of some of the calculation used below are close to those developed for droplets and capsules in the small deformation theory [11–13]. The function f is expanded in powers of ϵ and decomposed on the basis of spherical harmonics. In principle, it can be decomposed on an infinite series of spherical harmonics as

$$f = \sum_{n=0}^{+\infty} f_n \tag{3}$$

with $f_n=\Sigma_{m=-n}^{+n} a_{nm}(t)\mathcal{Y}_{nm}(\theta,\phi)$, where $\mathcal{Y}_{nm}$ are the usual spherical harmonics and a_{nm} are time-dependent amplitudes which are undetermined for the moment. We can alternatively write $f_n = F_{p_1,p_2,\ldots,p_n}\left[\frac{\partial^n r^{-1}}{\partial x_{p_1},\partial x_{p_2},\ldots,\partial x_{p_n}}\right] r^{n+1}|_{r=1}$ (where repeated indices are to be summed over). Most of our calculation is made with the second formulation. If only the leading order harmonics (second order, f_2, where we shall omit below the subscript since there is no source of confusion) are retained, as adopted here, we can write up to order ϵ^2 (where the superscript represents the order of the expansion in ϵ)

$$f = f^{(0)} + \epsilon f^{(1)} = F_{ij}^{(0)} Y_{ij} + \epsilon\left(-\frac{6}{5}F_{ij}^{(0)}F_{ij}^{(0)} + F_{ij}^{(1)}Y_{ij}\right) \tag{4}$$

with the zeroth and first order amplitudes $F_{ij}^{(0)}$ and $F_{ij}^{(1)}$, respectively, and the abbreviation

$$Y_{ij} = \left(\frac{\partial^2 r^{-1}}{\partial x_i \partial x_j}\right)_{r=1}, \quad r = (x_1^2 + x_2^2 + x_3^2)^{1/2}. \tag{5}$$

The $O(\epsilon)$ term $-6/5F_{ij}^{(0)}F_{ij}^{(0)}$ ensures constant volume.

As Y_{ij} is a second-order spherical harmonic, the tensors $F_{ij}^{(0)}$ and $F_{ij}^{(1)}$ have only five independent elements. We can thus demand that $F_{ij}^{(0)}$ and $F_{ij}^{(1)}$ are symmetric and traceless. In this case Eq. (4) can also be written as

$$f = \left[3F_{ij}^{(0)}x_i x_j + \epsilon\left(-\frac{6}{5}F_{ij}^{(0)}F_{ij}^{(0)} + 3F_{ij}^{(1)}x_i x_j\right)\right]_{r=1}. \tag{6}$$

In order to ensure that the excess area of the surface parametrized by Eq. (2) is ϵ^2, the five remaining coefficients $F_{ij}^{(0)}$ are not independent but coupled by the constraint

$$[F_{11}^{(0)}]^2 + [F_{22}^{(0)}]^2 + F_{11}^{(0)}F_{22}^{(0)} + [F_{12}^{(0)}]^2 + [F_{13}^{(0)}]^2 + [F_{23}^{(0)}]^2 = \frac{5}{96\pi}. \tag{7}$$

Equations (4) and (7) guarantee that the vesicle volume is $V=\frac{4}{3}\pi+O(\epsilon^3)$ and the vesicle surface area is $A=4\pi+\Delta+O(\epsilon^3)$. We shall see later that including the $F_{ij}^{(1)}$ guarantees the constraint of excess area up to ϵ^4.

Our ansatz includes spherical harmonics of order 2 only. It is justified by the fact that the external flow only contains harmonics of order 2. At next-to-leading order, modes of order 4 are excited, however, they do not couple back to the modes of second order. It is thus possible to derive a closed description that contains second-order spherical harmonics only. It is only at higher orders (not included here) that higher order harmonics may affect dynamics.

Next we compute, up to $O(\epsilon^2)$, the two tangential vectors

$$\mathbf{t}_\theta = \partial_\theta \mathbf{R}, \quad \mathbf{t}_\phi = \partial_\phi \mathbf{R}, \tag{8}$$

and the unit normal vector

$$\mathbf{n} = \frac{\mathbf{t}_\theta \times \mathbf{t}_\phi}{|\mathbf{t}_\theta \times \mathbf{t}_\phi|}. \tag{9}$$

From the tangential vectors follows the metrics

$$g_{ij} = \mathbf{R}_i \cdot \mathbf{R}_j \tag{10}$$

with its inverse g^{ij}. Following Seifert [2], we evaluate the curvature tensor

$$h_{ij} = (\partial_i \partial_j \mathbf{R}) \cdot \mathbf{n}, \tag{11}$$

which yields the mean curvature

$$H = \frac{1}{2} g^{ik} h_{ki} \tag{12}$$

and the Gaussian curvature

$$K = \det(g^{ik} h_{kj}). \tag{13}$$

In terms of the amplitudes of the shape function we have, for example,

$$H = -1 - 2\epsilon F_{ij}^{(0)} Y_{ij} - \epsilon^2 \left[\frac{6}{5} F_{ij}^{(0)} F_{ij}^{(0)} + 2F_{ij}^{(1)} Y_{ij} - 5F_{ij}^{(0)} F_{lm}^{(0)} Y_{ij} Y_{lm} \right] + O(\epsilon^3). \tag{14}$$

B. Velocity field

In common experiments, the Reynolds number of the flow is much smaller than unity. The dynamics of the flow is thus adequately described by the Stokes equations for the velocity field $\mathbf{u}$ and the pressure p,

$$\eta_\alpha \nabla^2 \mathbf{v} = \nabla p, \tag{15}$$

where η_0 is the viscosity of the suspending fluid and η_1 is the viscosity of the fluid inside. We define, as usual, the ratio $\lambda \equiv \eta_1 / \eta_0$. We can safely assume that the fluids are incompressible, and thus

$$\nabla \cdot \mathbf{v} = 0. \tag{16}$$

The total velocity field outside the vesicle can then be written as $\mathbf{v} = \mathbf{v}_0 + \mathbf{u}$, where $\mathbf{u}$ is the perturbation of the field due to the presence of the vesicle, and the imposed shear flow $\mathbf{v}_0$ is taken in the form $\mathbf{v}_0 = \dot{\gamma} x_2 \mathbf{e}_1$, where $\dot{\gamma}$ is the shear rate. Likewise, we write for the velocity field within the vesicle $\bar{\mathbf{v}} = \omega \times \mathbf{r}/2 + \bar{\mathbf{u}}$, where ω is the vorticity. Following Lamb [14], we write an ansatz for the unknown perturbation of the velocity field outside the vesicle in the form

$$\mathbf{u} = \sum_{n=0}^{\infty} \nabla \chi_{-n-1} \times \mathbf{r} + \nabla \phi_{-n-1} - \frac{n-2}{2n(2n-1)} r^2 \nabla p_{-n-1} + \frac{n+1}{n(2n-1)} \mathbf{r} p_{-n-1} \tag{17}$$

and, inside the vesicle,

$$\bar{\mathbf{u}} = \sum_{n=0}^{\infty} \nabla \bar{\chi}_n \times \mathbf{r} + \nabla \bar{\phi}_n + \frac{n+3}{2(n+1)(2n+3)} r^2 \nabla \bar{p}_n - \frac{n}{(n+1)(2n+3)} \mathbf{r} \bar{p}_n. \tag{18}$$

The first term expresses vortex motion in a uniform pressure field. The second term represents an irrotational motion which can exist in a uniform pressure field. The last two terms are connected with the pressure distribution.

The functions $\bar{p}_n$, $\bar{\phi}_n$, and $\bar{\chi}_n$ in the Lamb solution are solid spherical harmonics of order n and p_{-n-1}, ϕ_{-n-1}, χ_{-n-1} are solid spherical harmonics of order $-n-1$ [11]. Splitting off their r dependence, we write $\chi_{-n-1} = r^{-n-1} Q_n$, $\phi_{-n-1} = r^{-n-1} S_n$, and $p_{-n-1} = r^{-n-1} T_n$. Likewise for the quantities within the vesicle: $\bar{\chi}_n = r^n \bar{Q}_n$, $\bar{\phi}_n = r^n \bar{S}_n$, and $\bar{p}_n = r^n \bar{T}_n$. The precise values of the functions $Q_n, S_n, \ldots$ (which are surface spherical harmonics and thus depend only on the angles) are determined from the boundary conditions at the membrane, as will be seen later.

Since a shear flow induces a shape deformation from a sphere which involves only second order harmonics (i.e., $n=2$), only $\mathcal{Y}_{2m}$ is active [2,4]. The other modes are damped [7,11] to leading order. So we can write the Lamb solution for the full velocity field $\mathbf{v}$ as

$$\bar{\mathbf{v}} = \nabla \bar{\phi} + \frac{5}{42} r^2 \nabla \bar{p} - \frac{2}{21} \mathbf{r} \bar{p} + \dot{\gamma}/2 (x_2 \mathbf{e}_1 - x_1 \mathbf{e}_2), \tag{19}$$

$$\mathbf{v} = \nabla \phi + \frac{1}{2} \mathbf{r} p + \dot{\gamma} x_2 \mathbf{e}_x, \tag{20}$$

where we explicitly write the external shear flow for the outer field and its rotational component for the inner field. Since there is only the second harmonic, we have dropped the subscripts (as in the terms p_{-n-1}, p_n, which would produce p_{-3} and p_2) in order to simplify the notations. The ansatz functions are expanded in powers of ϵ:

$$\bar{\phi} = [\bar{S}_{ij}^{(0)} Y_{ij} + \epsilon \bar{S}_{ij}^{(1)} Y_{ij}] r^2, \tag{21}$$

$$\phi = [S_{ij}^{(0)} Y_{ij} + \epsilon S_{ij}^{(1)} Y_{ij}] r^{-3} \tag{22}$$

and

$$\bar{p} = [\bar{T}_{ij}^{(0)} Y_{ij} + \epsilon \bar{T}_{ij}^{(1)} Y_{ij}] r^2 + \bar{p}_0, \tag{23}$$

$$p = [T_{ij}^{(0)} Y_{ij} + \epsilon T_{ij}^{(1)} Y_{ij}] r^{-3}. \tag{24}$$

C. Stress balance

We now formulate the stress balance at the membrane. To this end we have to evaluate the stresses exerted by the membrane as well as the hydrodynamical stresses from the fluids on both sides of the membrane.

The normal force exerted by the membrane is given by the Helfrich force [2]

$$F_n = \kappa [2H(2H^2 - 2K) + 2\Delta_S H] - 2ZH. \tag{25}$$

H and K are the mean and the Gaussian curvature, respectively, and Δ_S is the Laplace-Beltrami operator. Here Z is a Lagrange multiplier which enforces local membrane area conservation. At zeroth order, the bracketed term in Eq. (25) vanishes since $H^2 = K^2 = 1$ and $\Delta_S H = 0$. It follows that, at leading order, the bending rigidity of the membrane is not involved. This is just a consequence of the formal expansion we have adopted. In order to arrive at a nontrivial solution at zeroth order, we formally require κ (and $\partial_t f$) to scale as ϵ^{-1}.

In order to make all ϵ dependencies explicit, we introduce $\bar{\kappa}=\epsilon\kappa$ and write

$$F_n = \epsilon^{-1}\bar{\kappa}[2H(2H^2-2K)+2\Delta_S H]-2ZH. \tag{26}$$

By the same token, the isotropic part of Z must scale as ϵ^{-1}. The angular part, however, turns out to be $O(1)$. Hence we decompose the Lagrange multiplier Z in the following way:

$$Z = \epsilon^{-1}(Z_0^{(0)}+\epsilon Z_0^{(1)})+Z_{ij}^{(0)}Y_{ij}+\epsilon Z_{ij}^{(1)}Y_{ij}. \tag{27}$$

The tangential force exerted by the membrane (due to its incompressibility) is

$$\mathbf{F}_t = (g^{11}\mathbf{t}_\theta + g^{21}\mathbf{t}_\phi)\partial_\theta Z + (g^{12}\mathbf{t}_\theta + g^{22}\mathbf{t}_\phi)\partial_\phi Z. \tag{28}$$

The fluid stresses are given by the hydrodynamical stress tensor

$$\sigma_{ij} = -p\delta_{ij}+\eta_0(\partial_i v_j+\partial_j v_i), \tag{29}$$

$$\bar{\sigma}_{ij} = -\bar{p}\delta_{ij}+\eta_1(\partial_i \bar{v}_j+\partial_j \bar{v}_i). \tag{30}$$

The full stress balance at the membrane thus reads

$$[(\sigma_{ij}-\bar{\sigma}_{ij})n_j+F_n n_i]\mathbf{e}_i+\mathbf{F}_t=0, \tag{31}$$

which has to be evaluated at $r=R(\theta,\phi,t)=1+\epsilon f$.

D. Membrane incompressibility and kinematic condition

Membrane local incompressibility entails that the projected divergence of the velocity field must vanish on the membrane

$$(\delta_{ij}-n_i n_j)\partial_i v_j = 0. \tag{32}$$

We have in addition to require continuity of the fluid velocities across the membrane

$$v_i = \bar{v}_i \tag{33}$$

as well as equality with the velocity of the membrane (if we do not account for any permeation across the membrane). The latter condition reads

$$\epsilon\partial_t f = n_i v_i, \tag{34}$$

if we neglect $O(\epsilon^2)$ terms [17] [the full kinematic relation should involve $|\nabla(r-f)|$ in the denominator of the left-hand side term].

III. SOLUTION AT ZEROTH ORDER

In this section we shall deal with the leading order solution as originally derived by one of us [4]. By leading order we mean to keep only the terms having (0) in their superscript (e.g., $F_{ij}^{(0)}$). We shall present in the next section the solution to the next order. Following Frankel and Acrivos [12], we determine the ansatz coefficients from the boundary conditions by performing surface integrals over the (spherical) vesicle. For example, the equation

$$\int (v_i^{(0)}-\bar{v}_i^{(0)})x_j d\Omega = 0, \tag{35}$$

which is an integral version of the continuity condition at zeroth order (actually a projection of the ith vector component on the subspace of first-order spherical harmonics), yields the five relations

$$\bar{T}_{ij}^{(0)} - T_{ij}^{(0)} + 10\bar{S}_{ij}^{(0)} = \frac{5}{3}e_{ij}. \tag{36}$$

Similarly, the integral

$$\int (v_p^{(0)}-\bar{v}_p^{(0)})x_p x_i x_j d\Omega = 0 \tag{37}$$

(which is just the projection of the radial velocity balance on the subspace of second-order spherical harmonics, but can also be understood as a projection of the ith component of the radial velocity on the subspace of first-order spherical harmonics) gives the equations

$$\frac{2}{7}\bar{T}_{ij}^{(0)} - T_{ij}^{(0)} + 4\bar{S}_{ij}^{(0)} + 6S_{ij}^{(0)} = \frac{2}{3}e_{ij}. \tag{38}$$

From the stress balance [Eq. (31)] we have, upon projection on the appropriate subspace,

$$\int [(\sigma_{iq}^{(0)}-\bar{\sigma}_{iq}^{(0)})n_q^{(0)} + (F_n^{(0)}-2Z_0^{(0)})n_i^{(0)} + \mathbf{F}_t^{(0)}\cdot\mathbf{e}_i]x_j d\Omega = 0, \tag{39}$$

which gives rise to

$$\lambda\bar{T}_{ij}^{(0)} + \frac{3}{2}T_{ij}^{(0)} + 10\lambda\bar{S}_{ij}^{(0)} = \frac{5}{3}e_{ij} + Z_{ij}^{(0)} - 4(Z_0^{(0)}+6\bar{\kappa})F_{ij}^{(0)} \tag{40}$$

and at the same time fixes

$$p_0 = \frac{2}{\epsilon}(Z_0^{(0)}+\epsilon Z_0^{(1)}). \tag{41}$$

Finally, evaluating the integral

$$\int [(\sigma_{pq}^{(0)}-\bar{\sigma}_{pq}^{(0)})n_q^{(0)} + (F_n^{(0)}-2Z_0^{(0)})n_p^{(0)} + \mathbf{F}_t^{(0)}\cdot\mathbf{e}_p]x_p x_i x_j d\Omega = 0, \tag{42}$$

we find

$$3T_{ij}^{(0)} - \frac{1}{7}\lambda\bar{T}_{ij}^{(0)} + 4\lambda\bar{S}_{ij}^{(0)} - 24S_{ij}^{(0)} = \frac{2}{3}e_{ij} - 2Z_{ij}^{(0)} - 4(Z_0^{(0)}+6\bar{\kappa})F_{ij}^{(0)}. \tag{43}$$

Equations (36), (38), (40), and (43) determine the values of $T_{ij}^{(0)}$, $\bar{T}_{ij}^{(0)}$, $S_{ij}^{(0)}$, and $\bar{S}_{ij}^{(0)}$ as a function of e_{ij}, $Z_0^{(0)}$, $Z_{ij}^{(0)}$, and $F_{ij}^{(0)}$.

Likewise, the angular components $Z_{ij}^{(0)}$ of the membrane tension are found from the surface integral over the projected divergence [Eq. (32)]

$$\int (\delta_{pq}-n_p^{(0)}n_q^{(0)})\partial_p v_q^{(0)} x_i x_j d\Omega = 0 \tag{44}$$

which yields

$$\frac{3}{7}\bar{T}_{ij}^{(0)} + 2\bar{S}_{ij}^{(0)} = 0. \tag{45}$$

Having obtained the velocity field as a function of the shape amplitudes $F_{ij}^{(0)}$ (and e_{ij}, $Z_0^{(0)}$), we employ the same strategy to fulfill the kinematic condition (34):

$$\int (\epsilon \partial_t f^{(0)} - n_p^{(0)} v_p^{(0)}) x_i x_j d\Omega = 0. \tag{46}$$

The result is a set of five equations that describe the dynamics of the amplitudes

$$\epsilon \partial_t F_{ij}^{(0)} = \frac{20 e_{ij}}{23\lambda + 32} - \frac{24(Z_0^{(0)} + 6\bar{\kappa})}{23\lambda + 32} F_{ij}^{(0)}. \tag{47}$$

For the time being we leave the isotropic part $Z_0^{(0)}$ of the membrane tension undetermined, and it will be dealt with later in this paper.

IV. SOLUTION AT FIRST ORDER

The solution at first order is obtained in the same way as the solution at zeroth order, this is why we shall not dwell upon this issue. However, we must now apply the boundary conditions at $r=R$ instead of $r=1$ (in order to incorporate consistently the desired order in ϵ). To this end, we employ a Taylor series expansion around $r=1$. For example, the velocity field becomes

$$v_i|_{r=1+\epsilon f} = \left[v_i^{(0)} + \epsilon f^{(0)} x_j \frac{\partial v_i^{(0)}}{\partial x_j} + \epsilon v_i^{(1)} \right]_{r=1} + O(\epsilon^2). \tag{48}$$

For the continuity condition we have to evaluate the integrals

$$\int \left(v_i^{(1)} - \bar{v}_i^{(1)} + f^{(0)} x_q \frac{\partial (v_i^{(0)} - \bar{v}_i^{(0)})}{\partial x_q} \right) x_i d\Omega = 0, \tag{49}$$

$$\int \left(v_p^{(1)} - \bar{v}_p^{(1)} + f^{(0)} x_q \frac{\partial (v_p^{(0)} - \bar{v}_p^{(0)})}{\partial x_q} \right) x_p x_i x_j d\Omega = 0. \tag{50}$$

Similar integrals are constructed for the first-order stress balance. The resulting equations allow for the determination of $T_{ij}^{(1)}$, $\bar{T}_{ij}^{(1)}$, $S_{ij}^{(1)}$, and $\bar{S}_{ij}^{(1)}$.

Membrane incompressibility (32) provides us with the expression of $Z_{ij}^{(1)}$, and from the kinematic condition (34) we find at first order the following evolution equations for the amplitudes:

$$\begin{aligned}\epsilon \partial_t F_{ij}^{(1)} = & -\frac{\omega_s}{2}(\epsilon_{psi} F_{pj}^{(0)} + \epsilon_{psj} F_{pi}^{(0)}) - \frac{24}{23\lambda + 32}[Z_0^{(1)} F_{ij}^{(0)} + (Z_0^{(0)} \\ & + 6\bar{\kappa}) F_{ij}^{(1)}] + \frac{4800}{7} \frac{\lambda - 2}{(23\lambda + 32)^2} \mathcal{S}d[F_{ip}^{(0)} e_{pj}] \\ & + \frac{288}{7} \frac{1}{(23\lambda + 32)^2} \mathcal{S}d[F_{ip}^{(0)} F_{pj}^{(0)}][(138\lambda + 192)\bar{\kappa} \\ & + (49\lambda + 136)(Z_0^{(0)} + 6\bar{\kappa})],\end{aligned} \tag{51}$$

where we have introduced the notation $\mathcal{S}d[b_{ij}] = \frac{1}{2}[b_{ij} + b_{ji} - \frac{2}{3}\delta_{ij} b_{ll}]$ and ω_s is the s-component of the vorticity vector. Note that this equation still contains the undetermined functions $Z_0^{(0)}(t)$ and $Z_0^{(1)}(t)$, which must be chosen such that the dynamics of the amplitudes comply with the available excess area relative to the sphere.

V. COMBINING ZEROTH AND FIRST ORDER SOLUTIONS

We now proceed by casting the solutions at zeroth order, Eq. (47), and at first order, Eq. (51), into a single equation. To this end, we set $F_{ij} = F_{ij}^{(0)} + \epsilon F_{ij}^{(1)}$ and $Z_0 = Z_0^{(0)} + \epsilon Z_0^{(1)}$. Thus we obtain a single evolution equation for the amplitudes F_{ij}:

$$\begin{aligned}\epsilon \frac{\mathcal{D} F_{ij}}{\mathcal{D} \bar{t}} = & \frac{20 \bar{e}_{ij}}{23\lambda + 32} - \frac{24(Z_0 + 6\epsilon C_a^{-1})}{23\lambda + 32} F_{ij} + \epsilon \left[\frac{4800}{7} \frac{\lambda - 2}{(23\lambda + 32)^2} \mathcal{S}d[F_{ip} \bar{e}_{pj}] \right. \\ & \left. + \frac{288}{7} \frac{(49\lambda + 136) Z_0 + (432\lambda + 1008)\epsilon C_a^{-1}}{(23\lambda + 32)^2} \mathcal{S}d[F_{ip} F_{pj}] \right].\end{aligned} \tag{52}$$

The quantity

$$\frac{\mathcal{D} F_{ij}}{\mathcal{D} \bar{t}} \equiv \partial_{\bar{t}} F_{ij} + \frac{1}{2}(\epsilon_{psi} F_{pj} + \epsilon_{psj} F_{pi}), \tag{53}$$

entering this equation, is the Jaumann derivative (note that we consider all the calculation in the advected frame of the vesicle, so that we have partial derivative instead of material derivative as is usually written in the Jaumann derivative). ϵ_{psj} is the Levi-Civita tensor. The Jaumann derivative can also be rewritten as

$$\frac{\mathcal{D} \mathbf{M}}{\mathcal{D} \bar{t}} = \partial_{\bar{t}} \mathbf{M} + \frac{1}{2}(\Omega \cdot \mathbf{M} - \mathbf{M} \cdot \Omega), \tag{54}$$

where Ω is the vorticity tensor. In Eq. (52) time is adimensionalized by $\dot{\gamma}^{-1}$, and $\bar{e}_{ij}$ by $\dot{\gamma}$. The capillary number C_a is defined as

$$C_a = \frac{\eta_0 \dot{\gamma} r_0^3}{\kappa} \equiv \tau \dot{\gamma}, \tag{55}$$

where τ is a typical time scale for the relaxation of the vesicle towards its equilibrium when the flow is set to zero. In some sense C_a can also be viewed as a measure of how far from mechanical equilibrium the vesicle is in the course of its shear induced motion.

We shall now determine the Lagrange multiplier Z_0 by imposing that the shape functions F_{ij} must comply with the available excess area. In terms of F_{ij}, the surface of the vesicle is given by

$$\begin{aligned} A &= 4\pi + \Delta + O(\epsilon^4) \\ &= 4\pi + \epsilon^2 \frac{96\pi}{5}(F_{11}^2 + F_{22}^2 + F_{11}F_{22} + F_{12}^2 + F_{13}^2 + F_{23}^2) \\ &\quad + O(\epsilon^4). \end{aligned} \tag{56}$$

Note that after recasting the zeroth- and first-order amplitudes into one amplitude, the surface area is conserved up to $O(\epsilon^4)$. This is a very important point, since problems with constraints always trigger higher order nonlinearities than those initially present in the physical problem [15].

Evaluating $\partial_t A = 0$ and substituting Eq. (52) for $\partial_t F_{ij}$, we find the expression for Z_0, which reads

$$Z_0 = \frac{(8\pi F_{12} - 6C_a^{-1}\epsilon) + \epsilon A_0}{1 + \epsilon B_0} \tag{57}$$

with the abbreviations

$$A_0 = \frac{8\pi[1200(\lambda - 2)C_0 - 31104(3\lambda + 7)\epsilon C_a^{-1} D_0]}{35(23\lambda + 32)},$$

$$B_0 = \frac{1728\pi(49\lambda + 136)D_0}{35(23\lambda + 32)},$$

which contain the following combinations of the amplitudes:

$$C_0 = F_{11}F_{12} + F_{22}F_{12} + F_{13}F_{23},$$

$$\begin{aligned} D_0 &= F_{11}F_{22}^2 - F_{11}F_{12}^2 + F_{22}F_{13}^2 + F_{11}F_{23}^2 + F_{11}^2 F_{22} \\ &\quad - 2F_{23}F_{12}F_{13} - F_{12}^2 F_{22}. \end{aligned}$$

VI. GENERAL COMMENTS AND COMPARISON WITH OTHER WORKS

Let us make some general comments. If we set formally $\epsilon = 0$ on the right-hand side of Eq. (52) and in Eq. (57), we obtain the following equation:

$$\epsilon \frac{\mathcal{D}F_{ij}}{\mathcal{D}\bar{t}} = \frac{20\bar{e}_{ij}}{23\lambda + 32} - \frac{192\pi}{23\lambda + 32}\frac{F_{12}F_{ij}}{\Delta}. \tag{58}$$

This is the evolution equation derived in Ref. [4] (where time is rescaled by $\dot{\gamma}^{-1}$), which we call "leading order theory." Note that even to this leading order the evolution equation is nonlinear. This nonlinearity is triggered by local membrane incompressibility. Note that this markedly differs from droplet [11,12] and capsule [13] theories where the leading order equations are linear. The nonlinearities induce bifurcations and lead to the three dynamical modes *TT*, *TB*, and *VB*.

In the leading order theory the membrane rigidity (or C_a) scales out from the evolution equation. Following Ref. [4], two groups [8,9] recently attempted to include higher order contributions beyond Eq. (58). The calculations presented by Lebedev *et al.* [8] and Noguchi and Gompper [8,9] do not seem to conform to our theory. Lebedev *et al.* [8] add in the Helfrich force the next order term, but they ignored the corresponding hydrodynamical response. As shown below the ignored terms are stronger than those retained. This not only induces quantitative differences, but it is also shown below that the so-called self-similarity [8] (in that the equations contain only two independent parameters) does not hold.

Noguchi and Gompper [9] retain the full Helfrich force (without truncation), but as Lebedev *et al.* [8] they did not take into account the corresponding hydrodynamic response. In addition, the authors combine, without justification, various ingredients: (i) leading order theory [4] for the amplitude of vesicle deformation in order to compute the hydrodynamical response, (ii) the full Helfrich force (without including the corresponding velocity field), (iii) the semiphenomenological Keller-Skalak [16] theory for the orientation angle of the vesicle; this last point will become more clear in the next section. It is not clear why the authors consider it worthwhile to use a leading order theory for the amplitude of deformation, but a semiphenomenological theory for the orientation angle.

It should be stressed that a consistent theory [Eq. (52)], as presented here, induces higher and higher nonlinearities due the constraint of a given available excess area. In Sec. VII we shall present the main results which follow from the full equation (52).

In order to compare more precisely with previous analyses, it is convenient to expand the evolution equation (52) in powers of F_{ij}. For that purpose, we admit that F_{ij} is small enough, albeit it is formally of order unity. This is *a priori* justified by the fact that due to the available excess area constraint (7) the sum of the amplitudes is $5/96\pi \ll 1$. The idea is to express F_{ij} in terms of the orientation angle and the amplitude of deformation. For that purpose we make use of the following identity:

$$\sum_{i,k=1,2,3} 3x_i x_k F_{ik}(t) = \sum_{m=-2}^{2} a_{2m}(t) \mathcal{Y}_{2m}(\theta, \phi) \tag{59}$$

(note that a_{2m} was called F_{2m} in Ref. [4]).

Then using $a_{22} = \mathcal{R} e^{-2i\psi}$ as in Ref. [4], ψ coincides with the orientation angle of the vesicles (Fig. 2) and $\mathcal{R}$ is the amplitude of deformation of the vesicle. Instead of using $\mathcal{R}$, and for the sake of comparison with [8] we use the variable Θ defined by $\mathcal{R}/2\epsilon = \cos\Theta$. We expand the full equation (52) in powers of F_{ij} and retain terms up to the higher (fifth) order in F_{ij} in a consistent manner. We then perform a straightforward conversion of variables in terms of ψ and Θ. We find for Θ and ψ the following equations (where now we use physical time instead of $\bar{t}$):

$$T\partial_t\Theta = -S\sin\Theta\sin 2\psi + \cos 3\Theta + \epsilon\Lambda_1 S\sin 2\psi(\cos 4\Theta + \cos 2\Theta) + \epsilon\Lambda_2 S\sin 2\psi\cos 2\Theta + \cdots, \quad (60)$$

$$T\partial_t\psi = \frac{S}{2}\left\{\frac{\cos 2\psi}{\cos\Theta}[1+\epsilon\Lambda_2\sin\Theta] - \Lambda\right\} + \cdots, \quad (61)$$

where we define

$$S = \frac{7C_a}{9}\frac{\sqrt{3}\pi}{\epsilon^2}, \quad (62)$$

$$T = \frac{7C_a}{720}\sqrt{10\pi}\frac{23\lambda+32}{\dot\gamma}, \quad (63)$$

$$\Lambda = \frac{1}{240}\sqrt{\frac{30}{\pi}}(23\lambda+32)\epsilon, \quad (64)$$

$$\Lambda_1 = \frac{1}{28}\sqrt{\frac{10}{\pi}}\frac{49\lambda+136}{23\lambda+32}, \quad (65)$$

$$\Lambda_2 = \frac{10}{7}\sqrt{\frac{10}{\pi}}\frac{\lambda-2}{23\lambda+32}, \quad (66)$$

and the ellipsis stands for higher other terms of the series. The first term on the right-hand side of Eq. (60) corresponds to the leading order theory presented in Ref. [4]. The first and second terms correspond to the situation treated in Ref. [8], where only the higher order contribution in the membrane bending force is included [8,9]. Taking the corresponding hydrodynamical response to the same order into account (as done here) induces significant changes. A new term, for example, is the third term on the right-hand side of Eq. (60) (proportional to Λ_1). This term is at least of the same order as $\cos 3\Theta$. Indeed, the term proportional to $\Lambda_1 S$ is of the order of $\Lambda_1 C_a/\epsilon$. If one has in mind a formal spirit (or a mathematical spirit, in that C_a is taken of order unity), then ϵ should be regarded as being small. In that case the neglected terms are of order $1/\epsilon$, and are much higher than the retained term in the Helfrich energy, namely, $\cos 3\Theta$ (which is of order 1). As a natural consequence of this, the so-called similarity equations (put forward in Ref. [8], in that the evolution equations contain only two independent parameters S and Λ; while T can be absorbed in a redefinition of time) does not hold. Indeed, we have three parameters, which are C_a, λ, and Δ, the excess area (or, equivalently, ϵ).

Note that even if we consider ϵ not too small (the situation is worse otherwise), we have a term proportional to C_a. If one has in mind a physical situation, then it is known that most experimental observations operate at C_a significantly larger than 1 [5,6], and that the neglected terms are therefore higher than those retained.

VII. RESULTS

Equation (52) constitutes our basic result that we shall analyze now. We first analyze the *TT* regime. Figure 3 presents the orientation angle as a function of λ and compares the results with previous studies. Instead of a square root singularity found for the leading order theory (and in the Keller-Skalak regime [16]), the angle crosses zero quasilinearly. A point which is worth mentioning is that the *TT* angle becomes negative before the solution ceases to exist (signature of the *TB* regime). Before the solution ceases to exist the *VB* mode takes place, as discussed below.

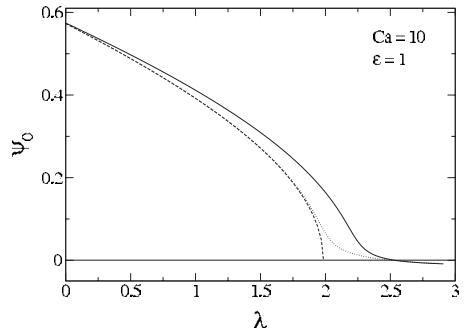

FIG. 3. The angle ψ_0 in the *TT* regime. Dashed line: the leading order theory [4], dotted line: the theory of Ref. [8], full line: the present theory.

In Ref. [4] it was predicted that in the tumbling regime a *VB* mode should take place. This was found to occur as an oscillator (as in a conservative system), since the frequency of oscillation about the fixed point $\psi=0$ was found to be purely imaginary. By including higher order terms the frequency acquires a nonzero real part [8], and the *VB* mode becomes a limit cycle [in that all initial conditions in its domain of existence tend towards a closed trajectory in phase space (ψ,Θ)]. As expected from the original theory [4] the *VB* mode still occurs in the vicinity of the tumbling threshold. This happens provided that the shape dynamics evolve with time (breathing of the shape). C_a is a direct measure for the comparison between the shape evolution time scale and the shearing time. The original theory [4] corresponds formally to $C_a\to\infty$, as can be seen from Eq. (60) and the definition of T and S. Including higher order terms leads to the appearance of C_a in the equation.

In Fig. 4 we report on the phase diagram and compare it to previous theories [4,8]. For small C_a we find, by increasing λ, a direct (saddle-node) bifurcation from *TT* to *TB*, in agreement with Ref. [3]. At $C_a\to\infty$ we recover the results of Ref. [4] (in that the *VB* mode coexists with *TB* and whether

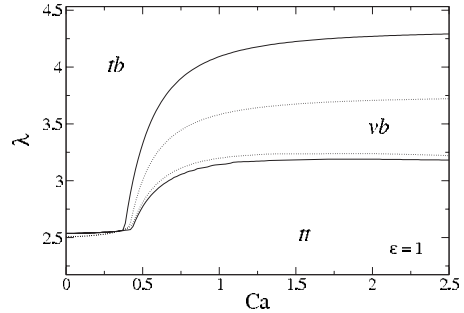

FIG. 4. The dotted line: theory in Ref. [8], full line: the present theory. The same order of discrepancy is found with Ref. [9].

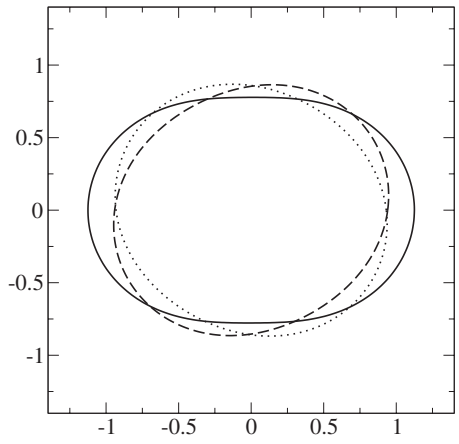

FIG. 5. A snapshot of the *VB* mode. Solid line: $\psi=0$. Dotted line: $\psi\simeq-0.5$. Dashed line $\psi\simeq0.5$. Parameters are $\epsilon=0.5$ and $\lambda=9$.

one prevails over the other depends on initial conditions; this is not shown in Fig. 2). At intermediate values of C_a we find a belt (or a domain) of the *VB* mode preceding the *TB* bifurcation, in qualitative agreement with Refs. [8,9], as shown in Fig. 4. For a given C_a and by increasing λ there is a bifurcation from the *TT* to *VB* which is of Hopf type (the imaginary part of the stability eigenvalue of the *TT* mode is imaginary). Once the *VB* appears, the *TT* still exists (but is unstable against *VB*). By further increasing λ one encounter the *TB* regime. This second transition corresponds to the fact that the *TT* mode ceases to exist.

The higher order calculation provided here shows significant differences with Refs. [8,9], as shown in Fig. 4. The results presented in Refs. [8,9] may be viewed as semiqualitative given the disregard of other terms of the same order, as commented in the previous section. Actually, a simplistic phenomenological model [17] captures the main essential qualitative features of Fig. 4.

Figure 5 shows a snapshot of the *VB* mode. Note that a pure swinging (a terminology usually used for oscillation of rigid objects, and adopted in Ref. [9]) would be impossible within the Stokes limit, since this is forbidden by the symmetry of the Stokes equation upon time reversal. The breathing is a necessary condition for the present mode. In the upper half plane (i.e., when $\psi>0$) the shape in the *VB* regime (dashed line in the figure) is different from the one in the lower plane (dotted line, rounded shape). This asymmetry makes this dynamics possible owing to the fact that the two shapes (i.e., for $\psi>0$ and $\psi<0$) can not be deduced from each other by a simple mirror symmetry with respect to the horizontal axis.

The basic understanding of the *VB* mode is as follows. First we recall that a shear flow is a sum of a elongational part along $\pm\pi/4$ (which elongates the vesicle for $\psi>0$ and compresses it for $\psi<0$) and a rotational part, tending to make a clockwise *TB*. Due to the membrane fluidity the torque associated with the shear is partially transferred to *TT* of the membrane, so that (due to torque balance) the equilibrium angle for *TT* is $0<\psi_0<\pi/4$. Furthermore, an elongated vesicle tumbles more easily than a compressed one [3]. Suppose we are in the *TT* regime ($\psi_0>0$), but in the vicinity of *TB*, so $\psi_0\simeq0$. For small C_a the vesicle's response is fast as compared to shear, so that its shape is adiabatically slaved to shear (a quasishape-preserving dynamics): a direct bifurcation from *TT* to *TB* occurs [3]. When $C_a\simeq1$, the shape does not adiabatically follow the shear anymore. When tumbling starts to occur ψ becomes slightly negative. There the flow compresses the vesicle. Due to this, the applied torque is less efficient. The vesicle feels, so to speak, that its actual elongation corresponds to the *TT* regime and not to *TB*. The vesicle returns back to its *TT* position, where $\psi>0$, and it now feels an elongation (which manifests itself on a time scale of the order of $1/\dot{\gamma}$). Due to elongation in this position, tumbling becomes again favorable, and the vesicle returns to $\psi<0$, and so on. We may say that the vesicle hesitates or vacillates between *TB* and *TT*. The compromise is the *VB* mode.

Finally it must be noted that experimentally it has not been possible to extract a phase diagram for the *VB* mode. In Ref. [6] it is stated (in Sec. 3.3) a small number of points correspond to an observed complex motion, denoted "transition motion…." In Ref. [5] the authors state shortly before the conclusion that at large C_a (χ in their notation) >10, and particularly in the close vicinity of the (*TB*) transition, a new type of motion was discovered. In both papers it has not been possible to be more precise. For example, when saying "in the close vicinity to the transition," it is not clear how close it must be. Referring to our Fig. 4, the distance (in the λ direction) between the *TT*-*VB* and *TB*-*VB* boundaries can be significant enough (for $C_a\sim2.5$, the two values of λ are of about 3.2 and 4.5, respectively). This is quite a significant difference. In addition, experimentally the shear rate (or C_a) was changed. So, if λ is chosen in the appropriate interval, then one could in principle observe the *VB* mode for a long period, and in a reproducible manner. We are aware, however, of the experimental difficulty (such as preparing an adequate desired viscosity ratio, together with the excess area) that this system presents. We hope that these questions will deserve more systematic attention in the future.

VIII. A BRIEF DISCUSSION OF RHEOLOGY

We briefly discuss the implication of the higher order theory on rheology. A complete discussion on this topic, and the comparison between droplets and capsules theory will be presented in the future.

Recently a link between the different modes and rheology has been presented [10]. It is thus natural to ask how higher order terms would modify the reported picture. Equation (52) constitutes a basis for the derivation of the constitutive law, as in Ref. [10]. Here we focus only on the effective viscosity as a function of λ. In the *TB* and *VB* regimes we make an average of the effective viscosity over a period of oscillation. The results are reported on Fig. 6.

We see that at small enough C_a, the cusp singularity (inset of Fig. 6) [10] persists as in the leading order theory, while at larger C_a the cusp is smeared out by the fact that the transition towards the *VB* mode does not show a singularity as does a saddle-node bifurcation.

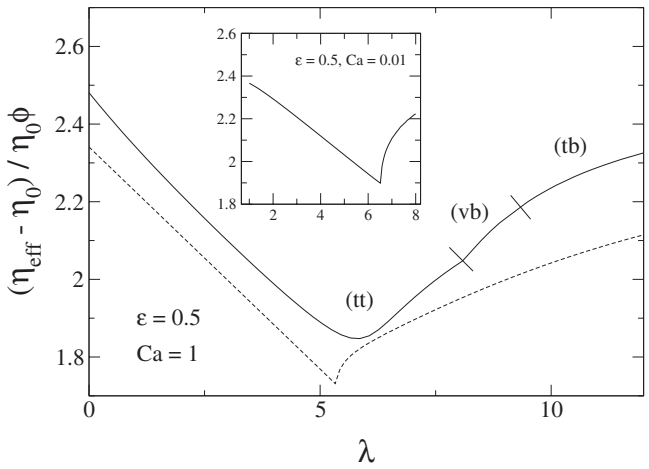

FIG. 6. The intrinsic viscosity is defined as $(\eta_{\text{eff}}-\eta_0)/\eta_0\phi$ (where ϕ is the vesicles volume fraction). The dashed line in the outer graph corresponds to the leading order theory where a cusp singularity is observed for any C_a. ϕ in the label of the vertical axis is the suspension volume fraction.

IX. DISCUSSION AND CONCLUSION

We have extended in a consistent manner the original theory [4] to higher order, and have analyzed the far reaching consequences. We have found that three parameters (i.e., the full set of dimensionless parameters that we can construct from the original model) survive to the next consistent leading order, thus ruling out some suspicions on self-similarity solutions, as announced in Ref. [8]. We have then analyzed the phase diagram of the evolution equation, and briefly discussed the behavior of the effective viscosity in the dilute regime. A particular point is that the next order terms wash out the cusp singularity of the effective viscosity [10] at the bifurcation point, provided that C_a is large enough. At low enough C_a the cusp singularity persists.

We have checked that for high enough $C_a \simeq 100$ (a quite accessible value in the experiments [6]) the full evolution equation produces a pseudocoexistence of the *VB* and *TB* solution. By "pseudo" we mean the following: if we start with an adequate initial condition (say ψ small), but the physical parameters are such that the *TB* mode should be expected from the phase diagram (Fig. 4), then the system can spend a long time in the *VB* regime (say about 50 cycles, or more; typically the number of cycles is of order $1/C_a$), before it falls onto the attracting mode, namely, the *TB* one. If, on the contrary, the *VB* mode is expected from the phase diagram, but the initial condition is such that ψ is large enough to enforce *TB*, then the system spends a long period of time in the *TB* regime before it exhibits *VB*. Since, to date, no systematic experimental study of the *VB* mode has been reported (the only reports show about two temporal periods [5,6]), our analysis shows that it may prove very difficult to locate experimentally the boundaries of the various modes, unless very clean and steady experimental conditions are produced.

Finally, this model has focused on vesicles. In order to make a step forward towards red blood cells, it is necessary to include the cytoskeleton structure, which is known to exhibit nonlinear viscoelasticity. Red cells exhibit some interesting dynamical behaviors [18]. We hope to tackle these questions along the present line of research in the future.

ACKNOWLEDGMENTS

G.D. and C.V. gratefully acknowledges support by the European Commission Marie Curie Research Training Network Grant No. MRTN-CT-2004-503661. C.M. and T.P. are grateful to CNES (Centre National d'Etudes Spatiales) and CNRS (ACI "mathématiques de la cellule et du myocarde") for financial support.

[1] M. Kraus, W. Wintz, U. Seifert, and R. Lipowsky, Phys. Rev. Lett. **77**, 3685 (1996).
[2] U. Seifert, Eur. Phys. J. B **8**, 405 (1999).
[3] T. Biben, C. Misbah, Phys. Rev. E **67**, 031908 (2003); J. Beaucourt, F. Rioual, T. Seon, T. Biben, and C. Misbah, *ibid.* **69**, 011906 (2004).
[4] C. Misbah, Phys. Rev. Lett. **96**, 028104 (2006).
[5] V. Kantsler and V. Steinberg, Phys. Rev. Lett. **96**, 036001 (2006).
[6] M. Mader, V. Vitkova, M. Abkarian, A. Viallat, and T. Podgorski, Eur. Phys. J. E **19**, 389 (2006).
[7] P. M. Vlahovska and R. S. Gracia, Phys. Rev. E **75**, 016313 (2007).
[8] V. V. Lebedev, K. S. Turitsyn, and S. S. Vergeles, e-print arXiv:cond-mat/0702650v1.
[9] H. Noguchi and G. Gompper, Phys. Rev. Lett. **98**, 128103 (2007).
[10] G. Danker and C. Misbah, Phys. Rev. Lett. **98**, 088104 (2007).
[11] G. Cox, J. Fluid Mech. **37**, 601 (1969).
[12] N. A. Frankel and A. Acrivos, J. Fluid Mech. **44**, 65 (1970).
[13] D. Barthès-Biesel, J. M. Rallison, J. Fluid Mech. **113**, 251 (1981); D. Barthès-Biesel and H. Sgaier, *ibid.* **160**, 119 (1985); A. Drochon, Eur. Phys. J. A **22**, 155 (2003).
[14] H. Lamb, *Hydrodynamics*, 6th ed. (Cambridge University Press, Cambridge, 1932).
[15] Suppose that we have a quantity, say a vector $\mathbf{m}$, whose norm must be constant in the course of time similar to a director in liquid crystals. In the harmonic approximation the vector $\mathbf{m}$ obeys a linear equation, say $\partial_t\mathbf{m}=L(\mathbf{m})$ where L is a certain linear operator. This equation does not conserve the norm of $\mathbf{m}$. In order to fulfill the constraint, we must add a term $\mu\mathbf{m}$ and write $\partial_t\mathbf{m}=L(\mathbf{m})+\mu\mathbf{m}$, where μ is a Lagrange multiplier enforcing constant norm of $\mathbf{m}$. Taking the scalar product with $\mathbf{m}$ and setting $\partial_t\mathbf{m}^2=\mathbf{0}$, determines μ and the final evolution equation becomes $\partial_t\mathbf{m}=L(\mathbf{m})-\mathbf{m}\cdot L(m)\mathbf{m}$. So the constrained equation has acquired a third nonlinearity, or in terms of energy, it has a quartic term, while the original nonconstrained energy is harmonic. This problem is somewhat akin to ours

where the evolution Eq. (52) acquires highly nonlinear terms hidden in Z_0.

[16] S. R. Keller and R. Skalak, J. Fluid Mech. **120**, 27 (1982).

[17] The qualitative features of vesicle dynamics taking into account deformability can be recovered in a straighforward manner. A simple phenomenological model can be built by coupling the Keller and Skalak [16] equation for ellipsoidal vesicles $\partial_t\psi=-\dot{\gamma}/2+B(r_2,r_3,\lambda)\cos 2\psi$, where r_2 and r_3 are the ellipsoid aspect ratios, to a phenomenological equation for the shape. This equation can be established by considering a balance between the internal viscous forces, a relaxation term due to membrane forces and external viscous forces. Using a little dimensional analysis, this yields $(\eta_0/r_2)\partial_t r_2=-(\kappa/R^3)\partial U/\partial r_2-\eta_1\dot{\gamma}\sin 2\psi$ or, equivalently, $\partial_t r_2=-(r_2/C_a\lambda)\partial U/\partial r_2-(r_2/\lambda)\sin 2\psi$. In this equation, C_a is the capillary number $C_a=\eta_o\dot{\gamma}R^3/\kappa$ and $U=\kappa\int H^2 ds$ is the Helfrich energy. A numerical resolution of this set of coupled equations yields phase diagrams which are qualitatively identical to the model presented in this paper or others [8,9].

[18] T. M. Fischer, Biophys. J. **86**, 3304 (2004); J. M. Skotheim and T. W. Secomb, Phys. Rev. Lett. **98**, 078301 (2007); M. Abkarian, M. Faivre, and A. Viallat, *ibid.* **98**, 188302 (2007).